

5-1-2023

Effects of different inlet configurations on the performance of solar storage tanks: A three-dimensional unsteady CFD simulation

Abdellah Shafieian
Edith Cowan University

Hamid Reza Bahrami

Amin Roostae

Seyed Sina Feyzi

Follow this and additional works at: <https://ro.ecu.edu.au/ecuworks2022-2026>



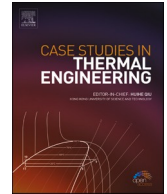
Part of the [Engineering Commons](#)

[10.1016/j.csite.2023.103019](https://doi.org/10.1016/j.csite.2023.103019)

Shafieian, A., Bahrami, H. R., Roostae, A., & Feyzi, S. S. (2023). Effects of different inlet configurations on the performance of solar storage tanks: A three-dimensional unsteady CFD simulation. *Case Studies in Thermal Engineering*, 45, 103019. <https://doi.org/10.1016/j.csite.2023.103019>

This Journal Article is posted at Research Online.

<https://ro.ecu.edu.au/ecuworks2022-2026/2391>



Effects of different inlet configurations on the performance of solar storage tanks: A three-dimensional unsteady CFD simulation

Abdellah Shafieian^{a,*}, Hamid-Reza Bahrami^b, Amin Roostaee^c, Seyed Sina Feyzii^d

^a School of Engineering, Edith Cowan University, 270 Joondalup Drive, Joondalup, Perth, WA, 6027, Australia

^b Department of Mechanical Engineering, Qom University of Technology, Qom, 37195, Iran

^c College of Engineering and Engineering Technology, Northern Illinois University, Still Gym 203, DeKalb, IL, 60115, USA

^d Independent Researcher

ARTICLE INFO

Handling Editor: Huihe Qiu

Keywords:

Thermocline
Storage tank
Solar
Thermal stratification
CFD simulation

ABSTRACT

A validated three-dimensional unsteady computational fluid dynamics analysis is performed in this study to investigate the effects of the inlet flow conditions on the thermal performance of solar storage tanks. First, effects of different mass flow rates on the thermal performance of a simple tank (Model 1, single inlet and single outlet) are investigated. The results show that higher mass flow rates deteriorate thermocline and thermal stratification which is desirable. To reduce the unfavorable effects of inlet jet mixing with stagnant fluid, the mass flow rates are divided equally between two inlet ports in the next model (Model 2). The results show that this model acts better than previous model from heat transfer point of view. In the next model (Model 3), the simple inlet port is replaced by a circular truncated cone shaped diffuser to reduce the momentum of the jet and impede unwanted mixing in the tank. The effects of the diffuser aspect ratio are analysed at fixed mass flow rates. The results reveal that small aspect ratios improve the performance of the tank while higher aspect ratios deteriorate the performance because of strongly adverse pressure gradient occurred inside the diffuser, which consequently results in a high-speed core flow, that contradicts with the idea of employing a diffuser. The outcomes indicate that only the aspect ratios between 1.0 and 1.5 have positive effects. In the final section, the study continues by modifying Model 3 through examining different orientations of the inlet port with respect to horizon (Model 4). Different angles including -30° , -15° , 15° , 30° are considered and the results show that changing inlet orientation is not as effective as the previous modifications.

Nomenclature

A_2/A_1	Area ratio
C_p	Specific heat of the fluid (J/kg.K)
g	Gravitational acceleration (m/s^2)
h	Inlet and outlet distance from base (m)
k	Thermal conductivity (W/m.K)
L	Tank height (m)
m	Mass flow rate (kg/s)

* Corresponding author.

E-mail address: a.shafieibandstjerdi@ecu.edu.au (A. Shafieian).

<https://doi.org/10.1016/j.csite.2023.103019>

Received 24 September 2022; Accepted 18 April 2023

Available online 22 April 2023

2214-157X/© 2023 The Authors. Published by Elsevier Ltd. This is an open access article under the CC BY-NC-ND license (<http://creativecommons.org/licenses/by-nc-nd/4.0/>).

P	Pressure (Pa)
Re	Reynolds number
t	Time(s)
T	Temperature(K)
$\frac{(T-T_{ini})}{T_{in}-T_{ini}}$	Dimensionless temperature
u	Velocity in x-direction (m/s)
z/L	Dimensionless height

Greek symbols

β	Thermal expansion coefficient (1/K)
ΔT	Difference between the outlet and inlet temperature ($^{\circ}C$)
τ	Stress tensor vector, (kg/m.s)
ρ	Density (kg/m^3)
θ	Inclination angle

Subscripts

in	inlet
ini	initial
out	outlet
ref	reference

1. Introduction

According to the increasing demand for energy and global warming problems, a lot of attention has been focused on harvesting renewable energies in recent years. Solar radiation as a sustainable and clean source of energy is available in many parts of the Earth. The main drawbacks of solar energy are its intermittency and instability. So, it is inconsistent with a stable demand from a heat load in different times of a day. Therefore, an extra device is needed to smooth the provided energy and match it with the heat load requirements. This apparatus is called a storage tank. Among different technologies for storage tanks, water-based and especially stratified ones achieved a great deal of popularity because of their simplicity and low cost [1,2]. These are the main reasons why research is still being conducted to improve this technology.

Amongst diverse designs, single stratified tank system is more widespread because they are simpler and cheaper than other configurations [3]. Stratification is physical phenomenon occurring inside a reservoir because fluids naturally tend to be stratified in a tank because of the buoyancy forces appearing due to different temperatures and subsequently dissimilar densities of different layers of the fluid [4]. However, due to multiple aims, it is desired to maintain or even boost the stratification phenomenon. During charge of the reservoir, mixing of the hot water jet provided by the collector and the cold water deteriorates the overall quality of energy supplied by reservoirs. It increases the temperature of feed water delivered by the reservoir (flows toward collector) and subsequently reduces solar energy absorption ability [5,6]. A cooler collector inlet flow (received from the bottom section of the storage tank) absorbs much energy than a warmer can.

The overall efficiency of a solar-assisted system and the quality of stratification in the storage tank are strongly interrelated [7,8]. Many experimental and numerical surveys have been carried out under different conditions and for many design factors to improve the stratification phenomenon. Investigations have shown that parameters including inlet flow conditions such as temperature or mass flow rate [9], inlet port conditions [10–12], geometry or aspect ratio of reservoir [13,14], location of hot water or cold water inlet/outlet [15], reservoir heat loss to surrounding [16,17], inlet/outlet flow rate [15], and conduction along the tank wall [18,19] have great impacts on the superiority of stratification.

Inlet flow velocity has a significant effect on retaining or disturbing the stratification phenomenon. High inlets with mass flow rate produce a jet with a high momentum which strikes the opposite wall before diffusing, which degrades thermal layers formation [15]. A study is done by ELSihy et al. [20], demonstrating that by increasing the inlet flow rate the thermocline thickness becomes thicker and consequently the heat storage/release period reduces. Dhahad et al. [21] presented a creative configuration, including two diffusers at the top and bottom of the a vertically cylindrical reservoir. Their results show that using this configuration could reduce turbulence in the tank and makes a thinner thermocline. Chandra and Matuska [22] presented a numerical investigation on effects of inlet conditions on the thermal stratification during discharge. They studied different inlet conditions including simple, slotted, and perforated inlets. The results of this study are interpreted using some non-dimensional numbers such as MIX and Richardson numbers. The investigation shows that the effect of inlet condition on the degree of stratification depends on the flow rate.

In low flow rates, different inlet conditions have nearly close performance while slotted inlet gives better results in higher inlet velocities. Kumar and Singh [23] performed a numerical study on a closed storage tank. The external flows pass inside tube bundles placed inside the reservoir. They validated their study against the experiment that they have done in the survey. Their results reveal that the degree of stratification depends on the location of the heat source inside the tank. Deng et al. [24] presented a new design for inlet and outlet of a reservoir. They are nonequal-diameter radial diffusers. They claimed that this concept could augment stratification inside the tank and simultaneously reduce material utilization with respect to conventional equal diffusers.

According to the review of literature, it can be observed that the performance of storage tanks depends on numerous factors and there are still so many challenging subjects in the design methodology that should be investigated. Furthermore, different investigations have usually concentrated on a single design. In this study, different configurations and locations for inlet port of a single stratified tank system during charge, including Model 1 (a single and simple inlet), Model 2 (double opposite inlets), Model 3 (single diffuser-shape inlet), and Model 4 (single inclined inlet) are considered. A three-dimensional unsteady analysis is done using the commercial software Ansys Fluent. The effects of different parameters including the charge time, inlet mass flow rate, aspect ratio of diffusers, and inlet orientation are studied. The performance of the models is compared. The results are presented using contours and curves.

2. Mathematical modeling

The geometry of the tank, as shown in Fig. 1, is precisely adopted based on the previous studies [25]. It is a cylindrical geometry with fixed height, H , and aspect ratio, $AR = 3.5$. The inlet is at h lower than the top base and it is located on the peripheral surface. The outlet port is situated at the same distance above the bottom base. Inlet and outlet ports are horizontally circular cylinder and may become circular-truncated cone (to act as a diffuser) or inclined. In diffuser cases, the inlet and outlet cross sections of diffusers are called A_1 and A_2 , respectively. In a part of this study, the inlet orientation with respect to horizon will be studied. The angle θ is the representative of this orientation. The exterior surfaces of the vessel are assumed insulated. Inlet temperature distribution and velocity magnitude are assumed uniform. The numeral settings of the tank geometry are given in the Result section.

To simplify the simulation, some extra assumptions are made. Working fluid, water, is incompressible and Newtonian, viscous dissipation and effects of pressure field on temperature field are neglected, and thermophysical properties of working fluid, excluding density, are constant. To account the buoyancy force, density is considered a temperature dependent parameter as follows [26]:

$$\rho(T) = 863 + 1.21 \times T - 0.00257 \times T^2 \quad (1)$$

The mass, momentum, and energy equations, used to solve thermal and hydrodynamic fields, could be simplified as follows [12]:
Mass:

$$\nabla \cdot u = 0 \quad (2)$$

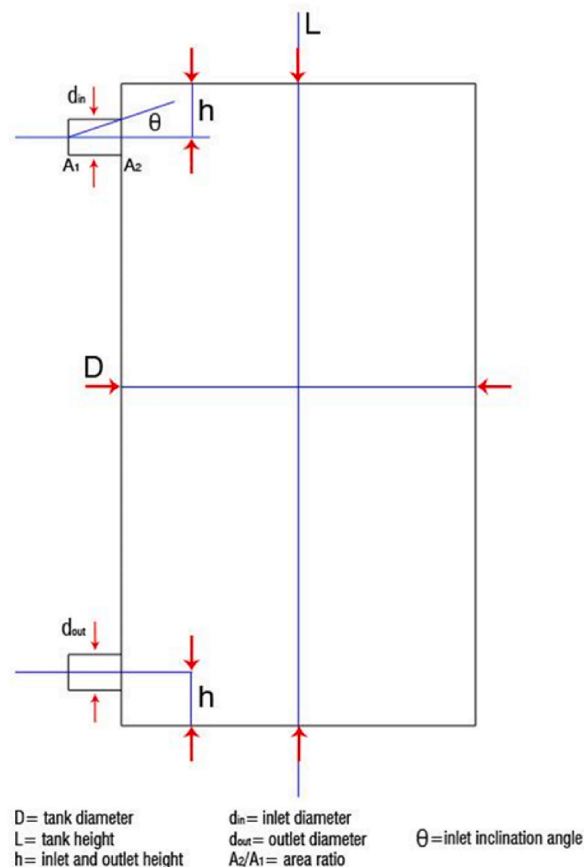


Fig. 1. Schematic of the geometry of the storage tank.

Momentum:

$$\rho \frac{\partial u}{\partial t} + (\rho u \cdot \nabla)u = -\nabla p + \nabla \cdot \tau - \rho\beta(T - T_{ref})g \tag{3}$$

Energy:

$$\rho C_p \frac{\partial T}{\partial t} + \rho C_p u \cdot \nabla T = \nabla \cdot (k \nabla T) \tag{4}$$

The last term in momentum equation is the source term added to account for the effects of buoyancy, based on the Boussinesq approximation [27].

The initial conditions for different velocity components and temperature are as follows:

$$u = v = 0; \quad T = T_{ini} = 60^\circ C \tag{5}$$

Velocity inlet and pressure outlet boundary conditions are applied to the inlet and outlet sections, respectively. Storage tank walls are adiabatic and no-slip condition is considered at all solid boundaries. The initial and inlet conditions as well as other geometry dimensions are given in Table z. According to the nature of the flow, the energy and flow equations are coupled. A pressure-based solver is selected to solve the governing equations. Pressure-velocity coupling is employed using SIMPLE algorithm [28], and the

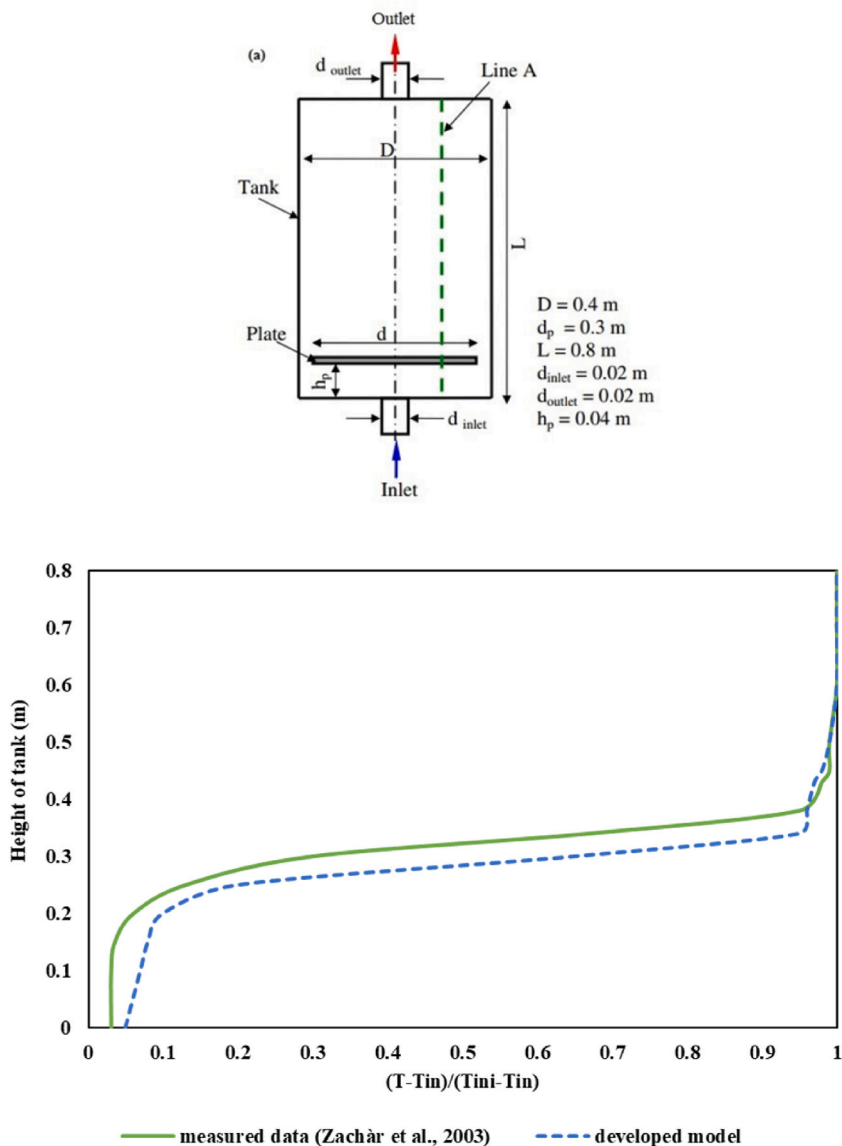


Fig. 2. (a) the configuration and dimensions of the experimental apparatus used in Ref. [29] and (b) Comparison of the current model and experimental results [29].

second order upwind discretization scheme is used for the convection terms. Furthermore, the solution is continued until the convergence criteria is met, where the residuals of all equations (other than continuity) fall below 10^{-6} and for continuity comes below 10^{-3} as well as changes in mass flow rates, temperature, and energy residuals become negligible.

The generated unstructured grid has a higher density of cells near the inlet and outlet positions, where important flow phenomena are expected. These cells should be small enough to capture the complex flow configuration. A grid independence test is performed to ensure the minimum influence of grid size on the results. Three different unstructured grids, successively refined (maximum, medium and fine meshes), are created using unstructured elements before setting 301,342–484,800 for the mesh sizes. As stated before, more cells were considered at inlet and outlet ports. Applying two inlets, Model 2 has the maximum number of cells.

2.1. Model validation

Experimental data published by Zachàr et al. [29] is used to validate the current numerical model. The configuration and dimensions of the tank used in that study are illustrated in Fig. 2a. The flow enters through the bottom vent and the passes through the gap between the tank and the metal plate. The hot water is harnessed at the top of the tank. Simulations are performed at inlet and initial temperatures of 20 °C and 41 °C, respectively and flow rate of 1.6 l/min. Temperature data along the line A (as shown in Fig. 2a, where thermocouples of the experiment were located) at time 1500s is compared. Fig. 2b illustrates the comparison between the current study and the results of Ref. [29]. It can be seen that there is a good agreement between the simulation and experimental results.

3. Results and discussion

In this section, different models are analysed. Model 1 is the basic model which its configuration is given Fig. 1. In the next section, Model 1 is modified so instead of one inlet, there are two inlets on the same level and in the opposite side. The modified model is called Model 2. The performance of Model 1 and Model 2 are compared in this section. In the following section, again, Model 1 is changed so that the simple inlet is replaced with a diffuser to reduce the inlet jet momentum. Next, in Model 4, the effect of diffuser (which is studied in the last model) orientation is studied. Settings for different modes are given in Table 1.

3.1. Model 1 (effect of mass flow rate)

In order to investigate the effects of the inlet mass flow rate on the thermal stratification within the tank, the base geometry with simple inlet and outlet ports, is considered. The initial temperature of water within the tank and the inlet water temperature are 30 °C and 60 °C, respectively. Simulations are performed for different mass flow rates; including 0.05, 0.1, and 0.15 kg/s. Fig. A1 shows the temperature distributions at times of 500s and 1000s. As it can be seen, the inlet water flows through the tank and hits the wall at the opposite side. In the way, until striking to the opposite boundary, it mixes with neighbour stagnant fluid and after striking it moves downward. As time is passing, a thermocline (an imaginary strip separating hot and cold zones where a steep temperature gradient occurs) forms and its thickness gradually increases which is due to the heat conduction within the line and mixing of upper layers. The thickness of the thermocline strip is an important factor determines how well the stratified tank is designed [30]. Increasing inlet flow rate results in more flow mixing due to the jet momentum and the buoyancy effects, which they expand the hot zone at the upper layer. Furthermore, it simultaneously decreases the average temperature of the hot region. With increasing flow rate, the inlet jet diffuses less through the stagnant region before it strikes strongly to the opposite side where the sturdy collision causes a greater mixing and adversely influences the diffusion. So, to achieve the optimum design, effects of both mixing and thermal diffusion within the tank is considered.

Fig. 3 shows the temperature profiles along the axis of the cylinder in different mass flow rates and charging times of 500s and 1000s. It can be observed that in lower mass flow rates, the dimensionless temperature drops more gradually toward the steady

Table 1
Setting of different cases studied.

Tests	Inclination Angle	L (mm)	D (mm)	H (mm)	M(kg/s)	A_2/A_1 ($A_1 = 0.0314 \text{ m}^2$)	T_{in} (C)	T_{ini} (C)	Number of inlets
Model 1	0	1194	341	20		1	60	30	1
Case 1					0.05				
Case 2					0.1				
Case 3					0.15				
Model 2	0	1194	341	20		1	60	30	2
Case 11					0.05				
Case 12					0.1				
Case 13					0.15				
Model 3	0	1194	341	20	0.1		60	30	1
Case 4						1.25			
Case 5						1.5			
Case 6						1.75			
Model 4		1194	341	20	0.1	1	60	30	1
Case 7	-15								
Case 8	15								
Case 9	-30								
Case 10	30								

conditions while it is steeper in higher mass flow rates. Increasing mass flow rate from 0.05 kg/s to 0.15 kg/s causes a greater mixing, lowers the average temperature of upper hot layers, and destroys the thermocline where all of them deteriorate thermal stratification.

3.2. Effect of applying double inlet port (model 2)

To improve the base model (discussed in the previous section), a new model, Model 2, is devised. In the new model, two similar inlet ports at opposite sides located on the opposite sides in the same level are considered. Subsequently, simulations are done for three different inlet mass flow rates and the results will be discussed at two instants 500s and 1000s. The main idea of the new design is to control inlet flow jet using to provide a better thermal stratification.

Simulation results, displayed in Fig. A2, show that the inlet jets collide around the axis and then disperse. It decreases momentum power and creates a region with higher average temperature around the top of the reservoir. In this model, sever temperature gradients are not created because of lower inlet flow rates as well as more continuous thermal distributions could be detected. As it is expected, the dimensionless temperature drops more slowly toward the steady state situation in lower values of mass flow rates while a steeper slope can be seen in higher mass flow rates. Furthermore, in smaller flow rates, the effect of buoyancy force is considerable, and the fluid stream tends to move upward. The main reason of heat transfer and thermocline growth is diffusion and mixing decreases. As the mass flow rate increases, the effect of mixing overcomes and consequently the thermocline grows faster. The temperature profiles along the axis of the chamber for different mass flow rates at charging time 500s and 1000s are shown in Fig. 4.

Fig. 5 shows the comparison of dimensionless temperature variation of Model 1 and Model 2 at three different mass flow rates and times of 500s and 1000s. The results prove that employing double inlet ports with lower flow rates does not have a significant effect on the temperature contours. As mass flow rate increases, the controlling inlet jet effect of applying double ports on thermocline formation and preservation becomes more evident, which leads to a better thermal stratification within the tank.

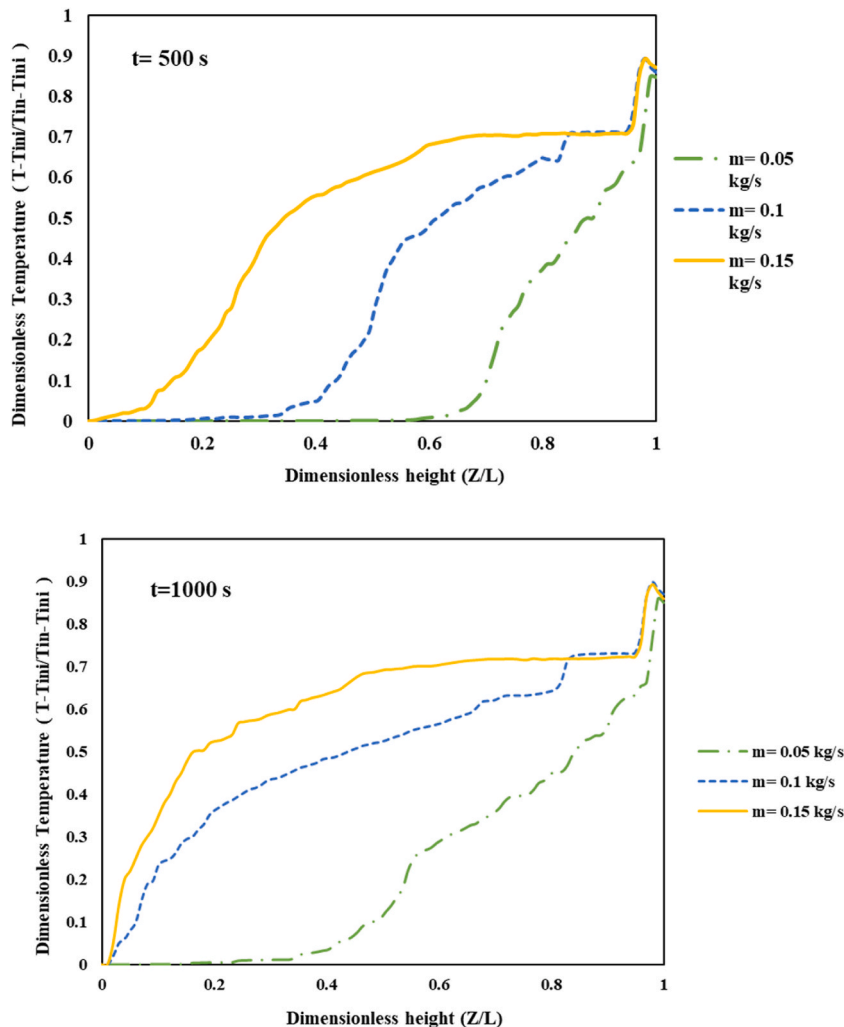


Fig. 3. Dimensionless temperature in different inlet mass flow rates along tank axis at 500s and 1000 s.

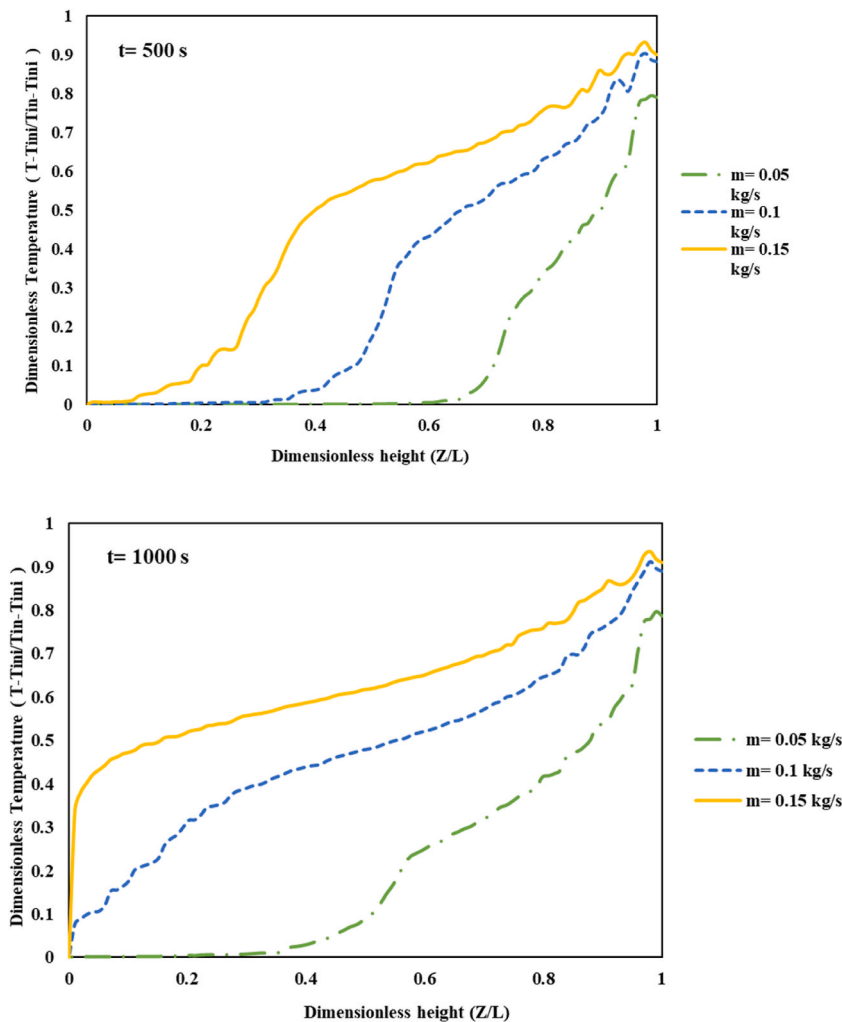


Fig. 4. Dimensionless temperature profile for tank with double inlets at different mass flow rates and times 500s and 1000s.

3.3. Effects of applying diffuser inlet ports (model 3)

In this section the effects of adding a diffuser in the inlet (in a single inlet tank) will be studied. The idea of using a diffuser is to decrease the flow velocity before entering the bulk of fluid and subsequently to improve the jet heat transfer with upper layers. Different aspect ratios of the diffuser, the ratio of the largest area to the smallest area (A_2/A_1), are used to study the effects of diffuser geometry on the thermal performance of the reservoir. This ratio is varied between 1.0 and 1.75 and mass flow rate is fixed at 0.1 kg/s. Fig. A3 shows the temperature contours in different conditions.

Considering Fig. 6, it can be seen that the flow pattern can be categorized according to the diffuser aspect ratio. For aspect ratios between 1.0 and 1.5, the diffuser causes a negative pressure gradient which reduces the nozzle outlet velocity. Accordingly, the lower inlet velocity results a slower flow jet, better buoyancy and diffusion effects and consequently a higher average temperature at the top section of the reservoir which gives a better thermal stratification. On the other hand, diffusers with aspect ratios greater than 1.5 result in recirculation zones inside the diffuser which are mainly due adverse pressure gradients occurring there. It reduces the active area inside the diffuser and a stronger core flow which has a high speed. So, a high-momentum hot flow enters the reservoir which causes more mixing and deteriorates buoyancy effects. Consequently, the average temperature of fluid locating above the jet decreases and simultaneously the average temperature in the bottom side also increases where both of them are not suitable for an ideal reservoir.

3.4. Effect of inlet inclination (model 4)

Another parameter which may affect the last configuration (Model 3) performance is diffuser orientation with respect to horizon. In this section, four different diffuser orientations (angles) are considered. Counter-clockwise angle is considered as negative angle and the clockwise one is positive. Effects of diffuser angle on the temperature distribution are given in Fig. A4. The main idea of using diffusers with negative angles is to control the inlet jet using the upper base of the tank as an obstacle where the collision of jet with

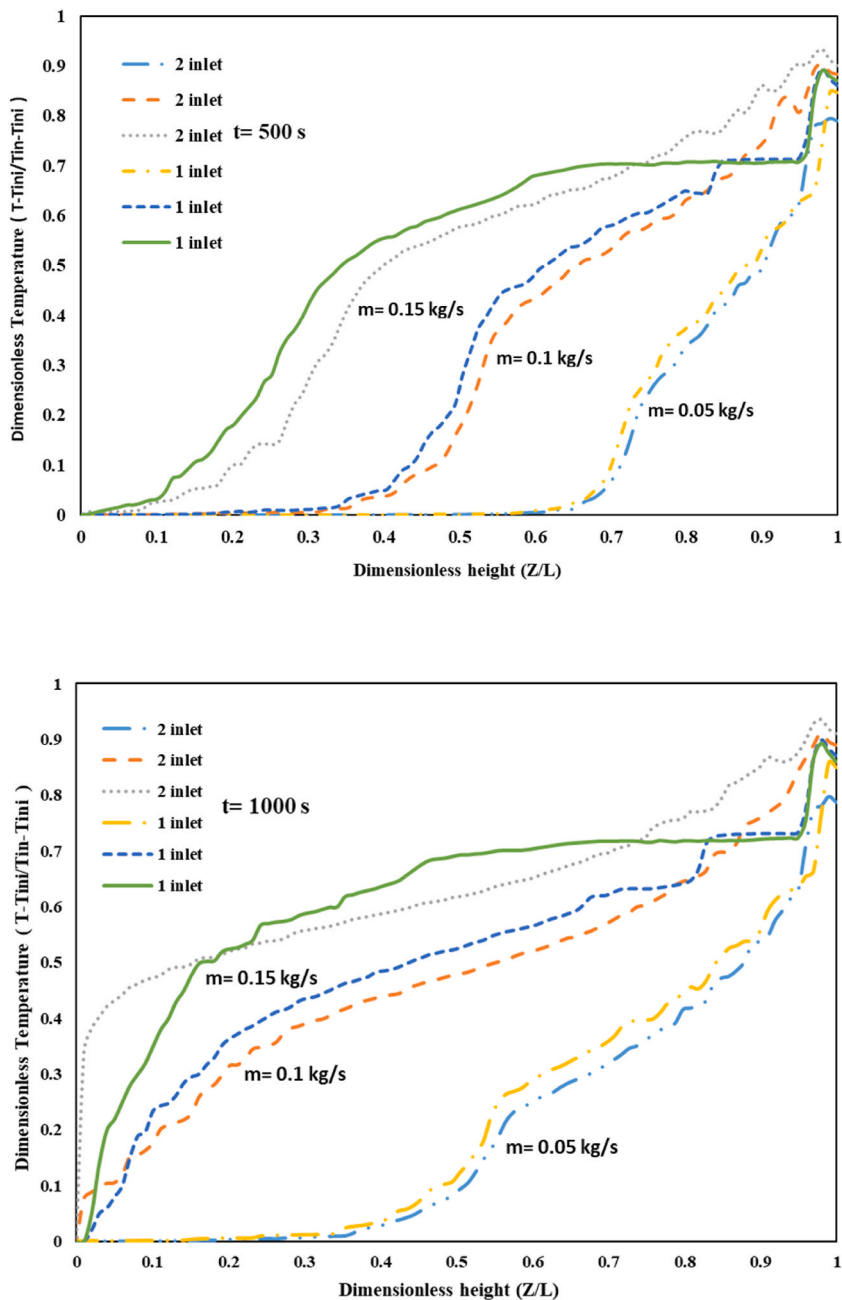


Fig. 5. Dimensionless temperature profiles for single and double inlet tanks at different mass flow rates and times 500s and 1000s.

upper base provides an extra time for diffusion mechanism. In the case of positive angles, the diffuser injects the inlet flow directly into the top layers which results in a great turbulence and more mixing. The detail of temperature variation through the axis of the reservoir for different conditions are given in Fig. 7. It can be observed that in the case of negative angles, the regions with maximum temperature are moved toward the upper base. Moreover, for negative angles, the thickness of the thermocline increases due to thermal diffusion and the effect of buoyancy force is negligible. On the contrary, positive angle causes direct penetration of hot fluid stream into lower layers, where mixing occurs noticeably. Therefore, it can be seen that thermocline grows significantly. Higher positive angles amplify buoyancy effects and strengthen heat transfer to the upper layers but increase mixing process which is not preferred.

Another noticeable point is that although the inlet orientation influences thermal distribution in the upper heights, its effects on the total thermal distribution are not considerable. The temperature profile of centre line for inlet inclination is lower than the usual inlet form and for higher negative angles is the lowest.

Fig. 8 illustrates the comparison of dimensionless temperature profiles of Model 3 and Model 4 (cases with positive angles) at mass

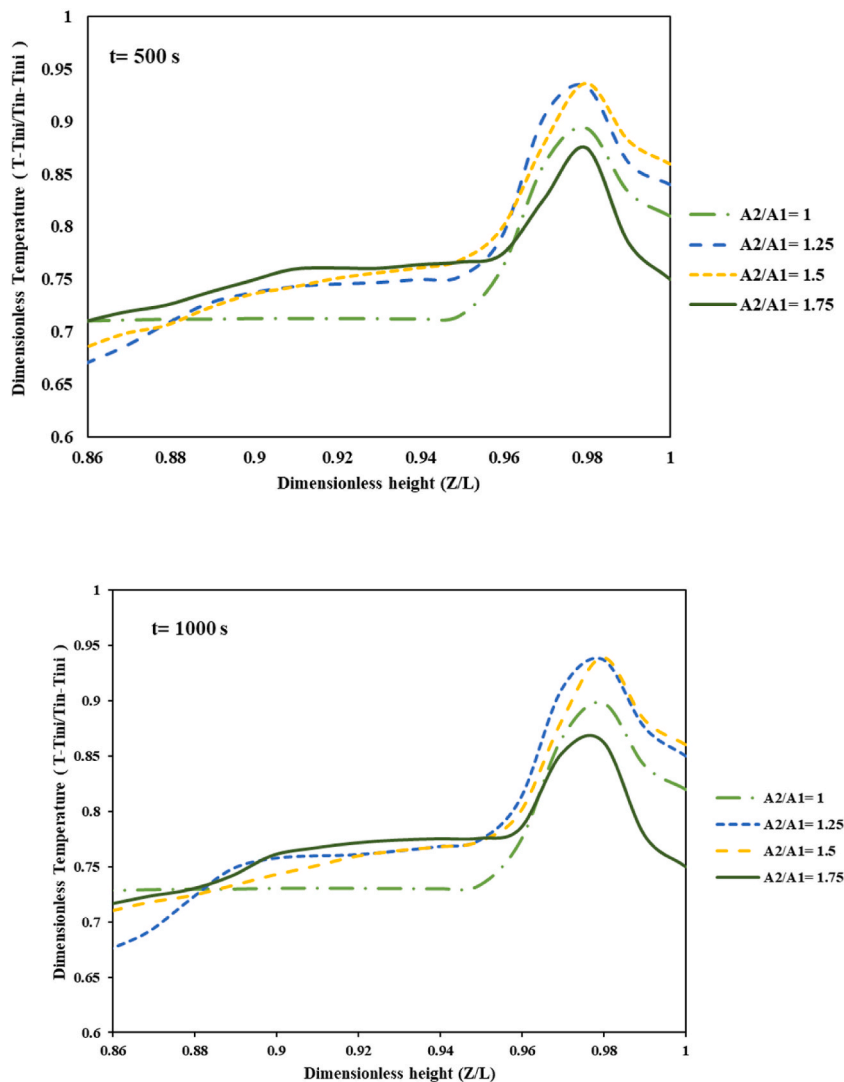


Fig. 6. Dimensionless temperature profiles for different aspect ratios at 500s and 1000s.

flow rate 0.1 kg/s and times 500s and 1000s. Results presented in the figure corroborate that applying diffuser inlet affects thermal distribution especially at upper heights more than inclined inlet, causing a greater thermal distribution along the tank.

4. Conclusion

In this study, 3D unsteady CFD simulations have been performed to investigate the effect of different inlet geometries (double inlet, diffuser, inclination) on thermal stratification in storage tanks for solar domestic hot water systems. The optimum values for the geometry of the tank were taken from previous studies. The proposed CFD model is validated against experimental. Simulations were run for different time of 500s and 1000 s. Results are analysed based on the effect of inlet flow jet on mixing (of hot jet and neighbour stagnant fluid), thermal diffusion, and buoyancy effects. First, a model with simple input (Model 1) is analysed. It can be concluded from simulation results that increasing inlet mass flow rate has a negative effect on thermal stratification within the tank. A higher flow rate means stronger jets that sturdily strikes the opposite side and destroys stratification. So, in order to keep the unwanted mixing as small as possible and to enhance thermal stratification, the inlet mass flow rates should be retained in low rates.

In the next model (model 2), double inlet on opposite section and in the same level as previous is considered. The collision of inlet streams, happening around the axis of the tank, reduces flow momentum and leads to a better thermal stratification. However, the improvement is negligible in small flow rates. Next, the inlet configuration is modified and a circular diffuser with different aspect ratios is considered with a fixed mass flow rate. Results show that diffusers with a small aspect ratio (smaller than 1.5) improve thermal performance while aspect ratios greater than this, due to reverse flow in the diffusers, deteriorate it. In Model 4, the orientation of the diffuser is changed between -30° and 30° . The results show that inlets with positive angles degrade thermal stratification.

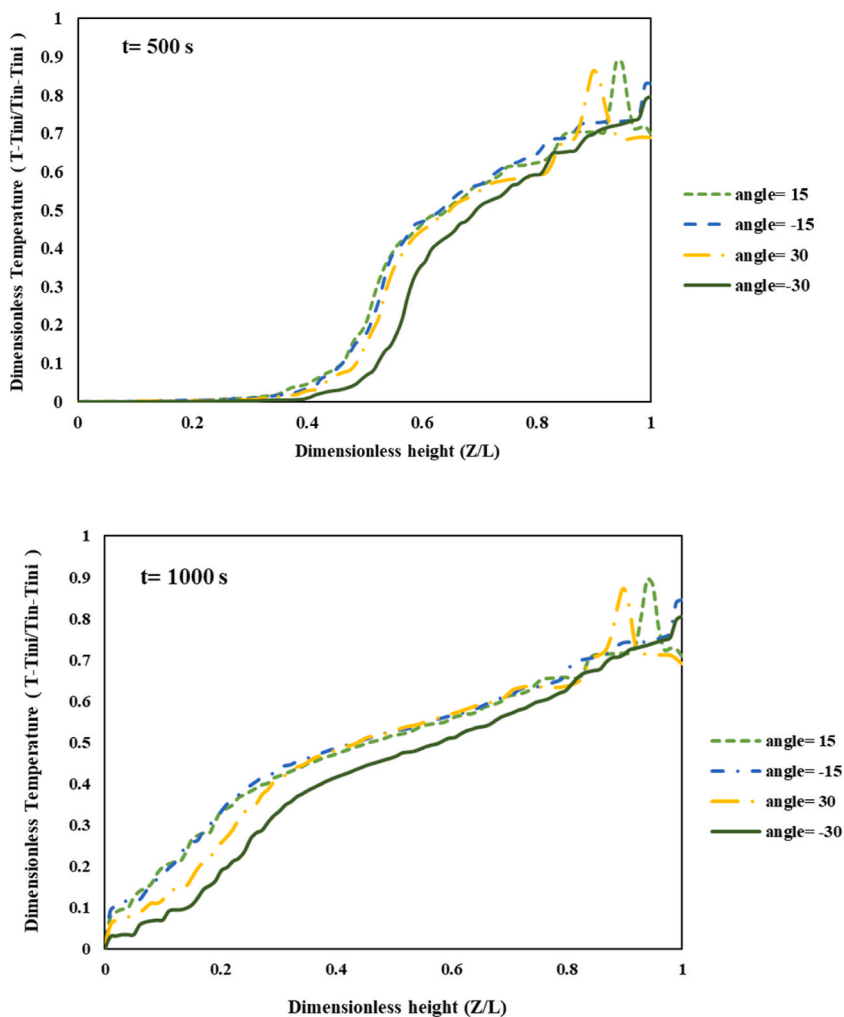


Fig. 7. Dimensionless temperature profile for inlet angles at time 500s and 1000s.

Declaration of competing interest

The authors declare that they have no known competing financial interests or personal relationships that could have appeared to influence the work reported in this paper.

Data availability

The authors are unable or have chosen not to specify which data has been used.

Appendix

A1. Model 1 (Effect of mass flow rate)

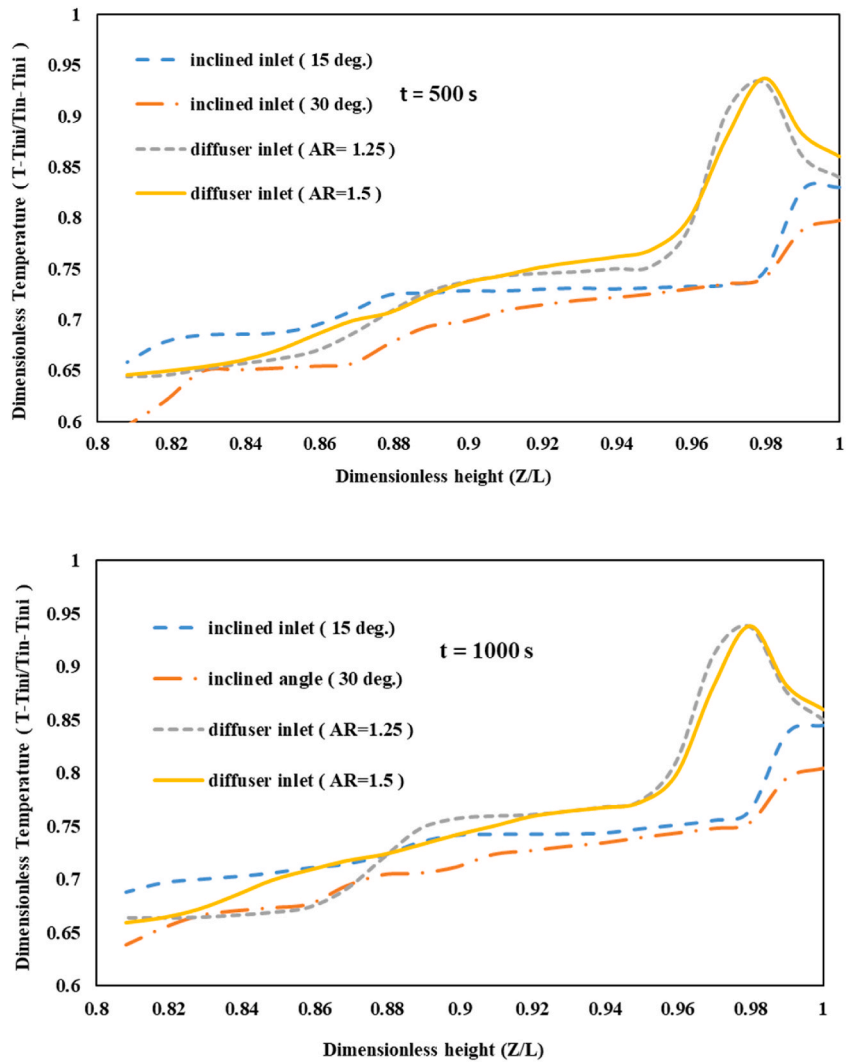


Fig. 8. Dimensionless temperature profiles for inclined and diffuser inlet tank at 500 and 1000 s.

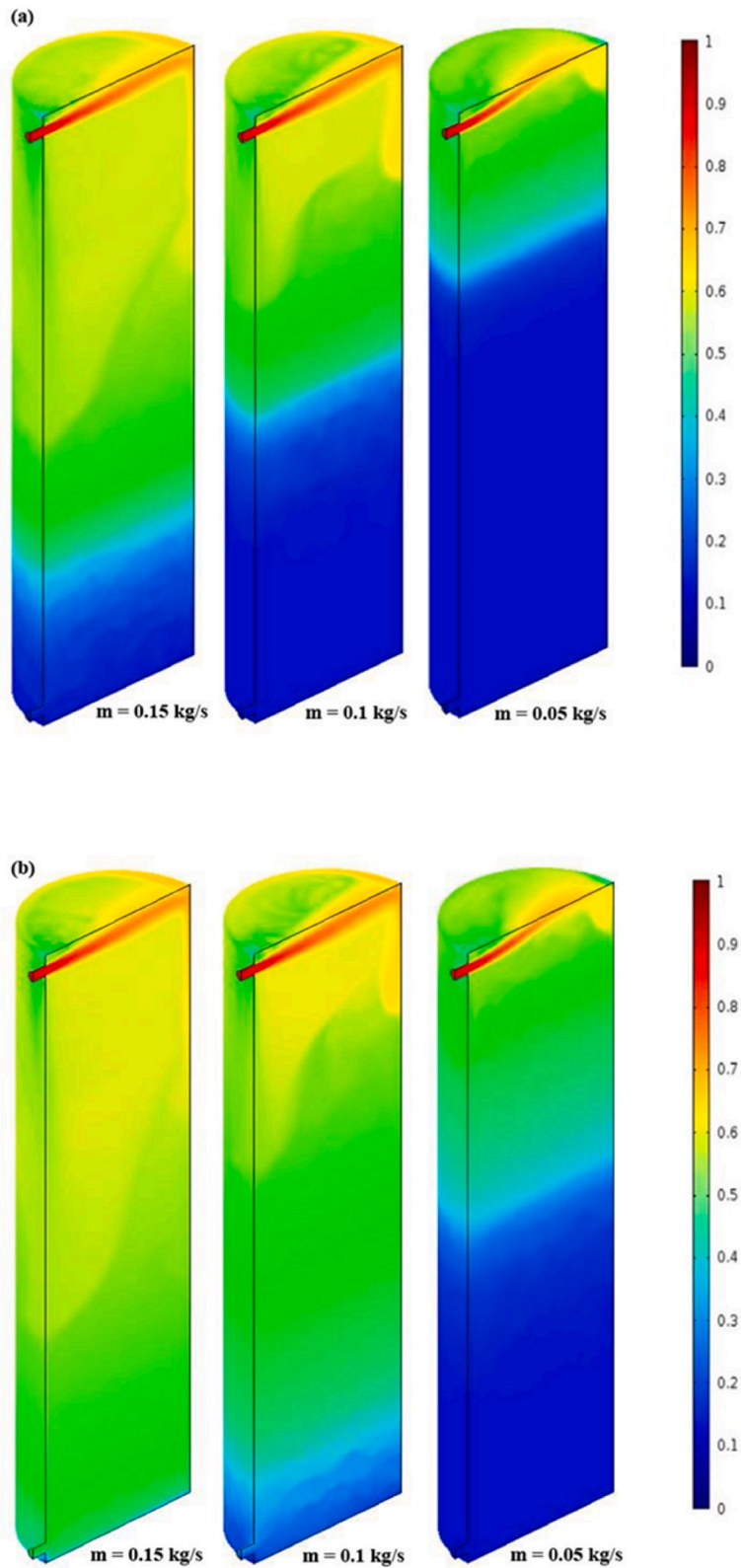


Fig. A1. Effects of mass flow rate on temperature contours: (a) $t = 500s$; (b) $t = 1000s$.

A2. Effect of applying double inlet port (Model 2)

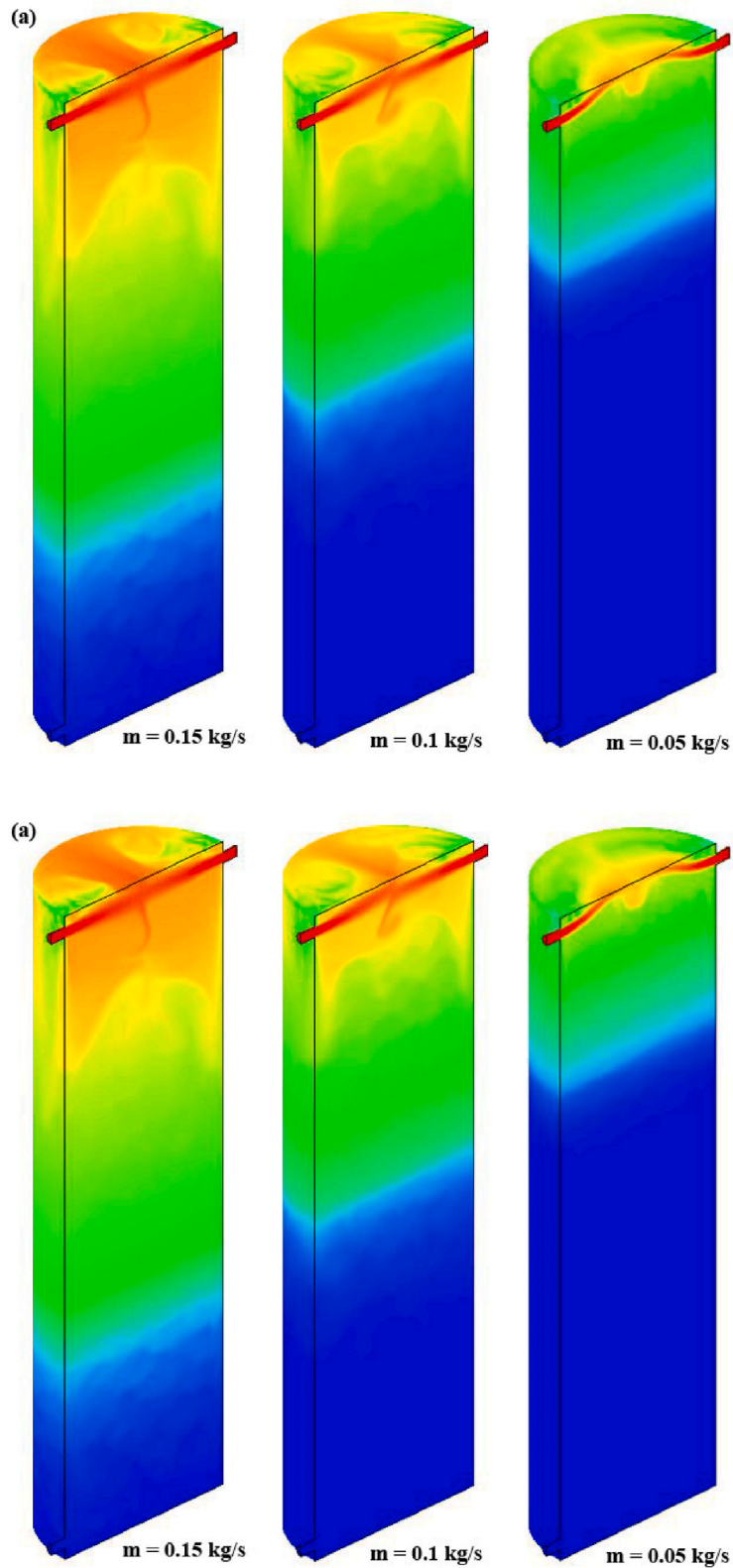


Fig. A2. Effects of applying double inlets on temperature profile at: (a) $t = 500s$; (b) $t = 1000s$.

A3. Effects of applying diffuser inlet ports (Model 3)

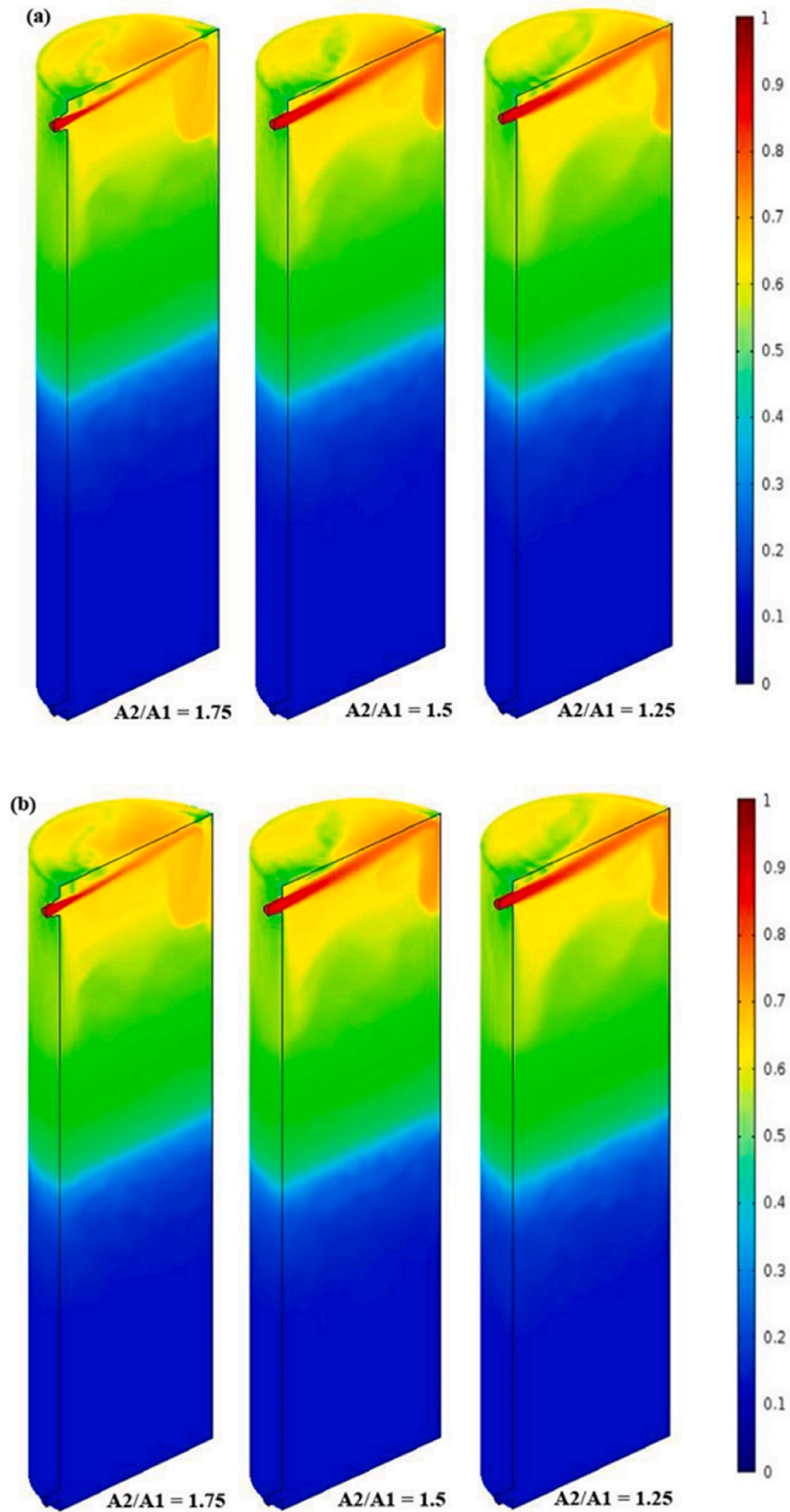


Fig. A3. Effects of employing a diffuser at the inlet of a single input reservoir on temperature contour at different times: (a) $t = 500s$, (b) $t = 1000s$.

A4. Effect of inlet inclination (Model 4)

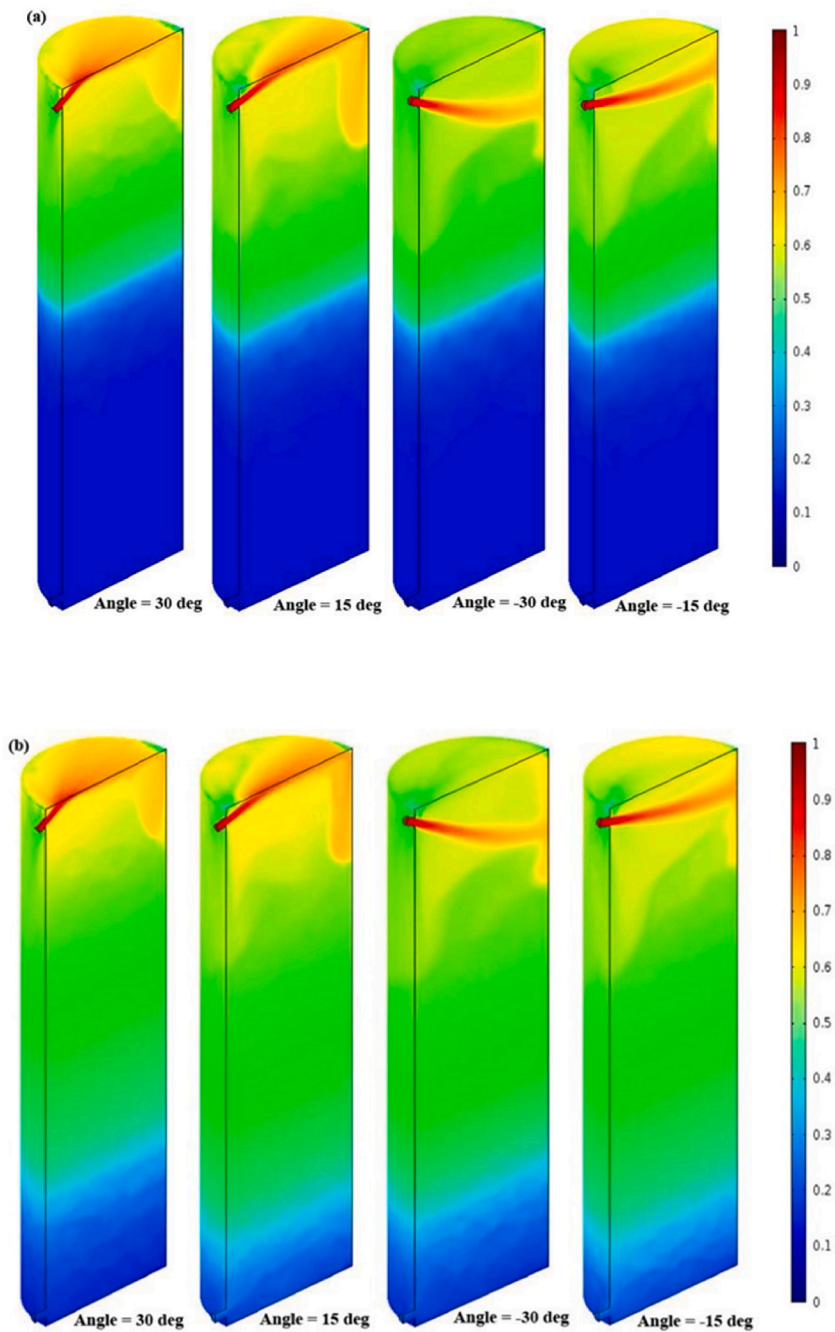


Fig. A4. Effect of applying double inlet on temperature contours: (a) $t = 00s$; (b) $t = 1000s$.

References

- [1] Y. Li, Y. Deng, M. Niu, et al., Surrogate modeling and optimization for the unequal diameter radial diffuser of stratified thermal energy storage tanks, *Energy Sci. Eng.* 10 (2022) 2497–2805.
- [2] S.M. Abd Elfadeel, H. Amein, M.M. El-Bakry, M.A. Hassan, Assessment of a multiple port storage tank in a CPC-driven solar process heat system, *Renew. Energy* 180 (2021) 860–873.
- [3] C.K.L. Sing, J.S. Lim, T.G. Walmsley, et al., Time-dependent integration of solar thermal technology in industrial processes, *Sustainability* 12 (2020) 2322.
- [4] V. Sb, S. Bhowmick, B.T. Kuzhiveli, Experimental and numerical investigation of stratification and self pressurization in a high pressure liquid nitrogen storage tank, *Energy Sources, Part A Recovery, Util. Environ. Eff.* 44 (2022) 2580–2594.

- [5] M.A. Gómez, J. Collazo, J. Porteiro, J.L. Míguez, Numerical study of an external device for the improvement of the thermal stratification in hot water storage tanks, *Appl. Therm. Eng.* 144 (2018) 996–1009, <https://doi.org/10.1016/j.applthermaleng.2018.09.023>.
- [6] Y.M. Han, R.Z. Wang, Y.J. Dai, Thermal stratification within the water tank, *Renew. Sustain. Energy Rev.* 13 (2009) 1014–1026, <https://doi.org/10.1016/j.rser.2008.03.001>.
- [7] M.Y. Haller, R. Haberl, P. Persdorf, A. Reber, Stratification efficiency of thermal energy storage systems – a new KPI based on dynamic hardware in the loop testing - Part I: test procedure, *Energy Proc.* 155 (2018) 188–208, <https://doi.org/10.1016/j.egypro.2018.11.056>.
- [8] J. Kalra, R. Pant, P. Negi, et al., Design optimization of solar thermal energy storage tank: using the stratification coefficient, in: *Machine Learning, Advances in Computing, Renewable Energy and Communication*, Springer, 2022, pp. 49–56.
- [9] C. Zhu, J. Zhang, Y. Wang, et al., Study on thermal performance of single-tank thermal energy storage system with thermocline in solar thermal utilization, *Appl. Sci.* 12 (2022) 3908, <https://doi.org/10.3390/app12083908>.
- [10] N.M. Brown, F.C. Lai, Enhanced thermal stratification in a liquid storage tank with a porous manifold, *Sol. Energy* 85 (2011) 1409–1417.
- [11] P. Trinuruk, P. Jenyongsak, S. Wongwiset, Comparative study of inlet structure and obstacle plate designs affecting the temperature stratification characteristics, *Energies* 15 (2022) 2032, <https://doi.org/10.3390/en15062032>.
- [12] A. Samet, M.A. Ben Souf, T. Fakhfakh, M. Haddar, Numerical investigation of the baffle plates effect on the solar water storage tank efficiency, *Energy Sources, Part A Recovery, Util. Environ. Eff.* 42 (2020) 2034–2048, <https://doi.org/10.1080/15567036.2019.1607925>.
- [13] A. Jamil, A. Benbassou, Review on solar thermal stratified storage tanks (STST): insight on stratification studies and efficiency indicators, *Sol. Energy* 176 (2018) 126–145.
- [14] M.T. Bouzaher, N. Bouchahm, B. Guerira, et al., On the thermal stratification inside a spherical water storage tank during dynamic mode, *Appl. Therm. Eng.* 159 (2019), 113821.
- [15] S. Ievers, W. Lin, Numerical simulation of three-dimensional flow dynamics in a hot water storage tank, *Appl. Energy* 86 (2009) 2604–2614.
- [16] P. Dzierwa, J. Taler, P. Peret, et al., Transient CFD simulation of charging hot water tank, *Energy* 239 (2022), 122241, <https://doi.org/10.1016/j.energy.2021.122241>.
- [17] B. Kurşun, Thermal stratification enhancement in cylindrical and rectangular hot water tanks with truncated cone and pyramid shaped insulation geometry, *Sol. Energy* 169 (2018) 512–525.
- [18] R.M. Dickinson, C.A. Cruickshank, S.J. Harrison, Charge and discharge strategies for a multi-tank thermal energy storage, *Appl. Energy* 109 (2013) 366–373.
- [19] A. Mawire, Parametric study on the thermal gradient of a small stratified domestic oil storage tank, in: *2016 International Conference on the Domestic Use of Energy (DUE)*, IEEE, 2016, pp. 1–5.
- [20] ELSihy ElsS, X. Wang, C. Xu, X. Du, Investigation on simultaneous charging and discharging process of water thermocline storage tank employed in combined heat and power units, *J. Energy Resour. Technol.* 143 (2020), <https://doi.org/10.1115/1.4047975>.
- [21] H.A. Dhahad, W.H. Alaweea, L.J. Habeeb, Numerical investigation for the discharging process in cold-water storage tank, *J. Mech.Res. Dev.* 43 (2020) 295–306.
- [22] Y.P. Chandra, T. Matuska, Numerical prediction of the stratification performance in domestic hot water storage tanks, *Renew. Energy* 154 (2020) 1165–1179, <https://doi.org/10.1016/j.renene.2020.03.090>.
- [23] K. Kumar, S. Singh, Investigating thermal stratification in a vertical hot water storage tank under multiple transient operations, *Energy Rep.* 7 (2021) 7186–7199, <https://doi.org/10.1016/j.egypr.2021.10.088>.
- [24] Y. Deng, D. Sun, M. Niu, et al., Performance assessment of a novel diffuser for stratified thermal energy storage tanks – the nonequal-diameter radial diffuser, *J. Energy Storage* 35 (2021), 102276, <https://doi.org/10.1016/j.est.2021.102276>.
- [25] W. Yaïci, M. Ghorab, E. Entchev, S. Hayden, Three-dimensional unsteady CFD simulations of a thermal storage tank performance for optimum design, *Appl. Therm. Eng.* 60 (2013) 152–163.
- [26] I. Editor, CFD simulation of SDHW storage tank with and without heater, *Int. J. Adv. Res. Technol - IJOART* (2012) 124–134.
- [27] R.D.C. Oliveski, A. de Quadro Tacques Filho, I.A. Schröer, Melting and solidification in thermal storage: influence of fin aspect ratio and positioning in a full charging and discharging cycle, *J. Energy Storage* 50 (2022), 104303, <https://doi.org/10.1016/j.est.2022.104303>.
- [28] C.-J. Hsu, Numerical heat transfer and fluid flow, *Nucl. Sci. Eng.* 78 (1981) 196–197, <https://doi.org/10.13182/NSE81-A20112>.
- [29] A. Zachár, I. Farkas, F. Szlivka, Numerical analyses of the impact of plates for thermal stratification inside a storage tank with upper and lower inlet flows, *Sol. Energy* 74 (2003) 287–302, [https://doi.org/10.1016/S0038-092X\(03\)00188-9](https://doi.org/10.1016/S0038-092X(03)00188-9).
- [30] A.M. Bonanos, E.V. Votyakov, Sensitivity analysis for thermocline thermal storage tank design, *Renew. Energy* 99 (2016) 764–771, <https://doi.org/10.1016/j.renene.2016.07.052>.